separations

MDPI

Article

Improved Expression of Aggregation-Prone Tau Proteins Using a Spidroin-Derived Solubility Tag

Kevin Muwonge [1,2,*], Bedri Yaman [1,2], Attila Mészáros [1,2], Giorgio Russo [1,2], Alexander Volkov [1,3] and Peter Tompa [1,2,4,*]

[1] VIB-VUB Center for Structural Biology, Vlaams Instituut voor Biotechnologie (VIB), 1050 Brussels, Belgium; bedri.batuhan.yaman@vub.be (B.Y.); attila.meszaros@vub.be (A.M.); giorgio.russo@vub.be (G.R.); oleksandr.volkov@vub.be (A.V.)
[2] Structural Biology Brussels (SBB), Vrije Universiteit Brussel (VUB), 1050 Brussels, Belgium
[3] Jean Jeener NMR Centre, Vrije Universiteit Brussel (VUB), Pleinlaan 2, 1050 Brussels, Belgium
[4] HUN-REN Research Centre for Natural Sciences, Institute of Molecular Life Sciences, 1117 Budapest, Hungary
* Correspondence: kevin.muwonge@vub.be (K.M.); peter.tompa@vub.be (P.T.)

Abstract: Tauopathies, a group of neurodegenerative disorders, are characterized by the abnormal aggregation of microtubule-associated Tau proteins in neurons and glial cells. The process of Tau proteins transitioning from soluble, intrinsically disordered monomers to disease-associated aggregates is still unclear. Investigating these molecular mechanisms requires the reconstitution of such processes in cellular and in vitro models using recombinant proteins at high purity and yield. However, the production of phase-separating or aggregation-prone recombinant proteins like Tau's hydrophobic-rich domains or disease mutation-carrying variants on a large scale is highly challenging due to their limited solubility. To overcome this challenge, we have developed an improved strategy for expressing and purifying recombinant Tau proteins using the major ampullate spidroin-derived solubility tag (MaSp-NT*). This approach involves using NT* as a fusion tag to enhance the solubility and stability of expressed proteins by forming micelle-like particles within the cytosol of *E. coli* cells. We found that fusion with the NT* tag significantly increased the solubility and yield of highly hydrophobic and/or aggregation-prone Tau constructs. Our purification method for NT* fusion proteins yielded up to twenty-fold higher amounts than proteins purified using our novel tandem-tag (6xHis-SUMO-Tau-Heparin) purification system. This enhanced expression and yield were demonstrated with full-length Tau (hT40/Tau441), its particularly aggregation-prone repeat domain (Tau-MTBR), and Frontotemporal dementia (FTD)-associated mutant (Tau-P301L). These advancements offer promising avenues for the production of large quantities of Tau proteins suitable for in vitro experimental techniques such as nuclear magnetic resonance (NMR) spectroscopy without the need for a boiling step, bringing us closer to effective treatments for tauopathies.

Keywords: solubility tag; spider silk protein; aggregation-prone; recombinant protein expression; protein purification; tauopathies; tau protein

check for updates

Citation: Muwonge, K.; Yaman, B.; Mészáros, A.; Russo, G.; Volkov, A.; Tompa, P. Improved Expression of Aggregation-Prone Tau Proteins Using a Spidroin-Derived Solubility Tag. *Separations* **2024**, *11*, 198. https://doi.org/10.3390/separations11070198

Academic Editor: Othman Al Musaimi

Received: 3 June 2024
Revised: 22 June 2024
Accepted: 23 June 2024
Published: 25 June 2024

Copyright: © 2024 by the authors. Licensee MDPI, Basel, Switzerland. This article is an open access article distributed under the terms and conditions of the Creative Commons Attribution (CC BY) license (https://creativecommons.org/licenses/by/4.0/).

1. Introduction

Tauopathies represent a group of neurodegenerative disorders characterized by abnormal Tau protein aggregation in both neurons and glial cells. This heterogeneous group includes nine confirmed members, with Alzheimer's disease (AD) and Frontotemporal Dementia (FTD) accounting for a large majority of dementia cases globally [1]. The process of Tau proteins transitioning from soluble, intrinsically disordered monomers to disease-associated aggregates (neurofibrillary tangles in AD and amorphous inclusions in FTD) is still unclear and a subject of intense research in the field of neurodegeneration [2,3]. The recently discovered cellular process of liquid–liquid phase separation (LLPS) is suspected to contribute to Tau's physiological functions as well as phase transitions that result in

its aggregation under pathological conditions [4–6]. Tau behaves as an intrinsically disordered protein (IDP) [7] in solution, necessitating the use of advanced techniques for its structural characterization, such as nuclear magnetic resonance (NMR) and single-molecule Förster Resonance Energy Transfer (smFRET) spectroscopy [8,9]. These techniques require large amounts of high-quality protein preparations produced and purified from bacterial expression systems.

The production and purification of recombinant proteins at high purity and yield are crucial for academic research and industrial applications [10]. In the pharmaceutical industry, biopharmaceuticals produced and purified as recombinant proteins are taking center stage to curb the growing need for more bioactive products on the market [11]. Similarly, expressed and purified recombinant proteins are used in practically all molecular and structural biology applications such as NMR, X-ray crystallography, cryo-electron microscopy (cryo-EM), and small-angle X-ray scattering (SAXS), which require substantially larger amounts of high-quality protein [12,13]. Consequently, researchers are investing considerable effort into developing enhanced methods for producing and purifying recombinant proteins [14,15]. While the host organism used for recombinant protein expression dictates the purification strategy, the downstream application of the purified protein dictates the choice of expression system used [16–18]. Bacterial expression systems are favored when copious amounts of recombinant proteins are required. These systems have proven to be cost effective and easy to handle, and their use follows well-established protocols [19]. However, these systems cannot perform the typical post-translational modifications (PTMs) that are essential to achieving the native and functional states of eukaryotic proteins [20]. Furthermore, removing bacterial endotoxins from samples can be challenging, potentially hindering specific biotechnological applications [21]. Bacterial systems may also struggle to produce soluble proteins, as many proteins with low solubility or aggregating tendencies sequester in bacterial inclusion bodies (IBs) [22,23].

Escherichia coli (*E. coli*) is the most common host organism used for recombinant protein production [24]. As an expression system, *E. coli* is easy to manage, cost effective, grows rapidly, and typically produces large quantities of the desired recombinant protein [25]. However, the lack of PTMs characteristic of eukaryotes on expressed recombinant proteins could hamper the proper folding of structural proteins or increase aggregation propensities of hydrophobic regions, especially those residing in IDPs that lack well-defined 3D structures [7,17,26]. *E. coli* circumvents the toxicity associated with aggregation-prone polypeptides massively produced in its cytoplasm by inclusion body formation [22]. But sequestering expressed recombinant proteins in IBs presents additional challenges in terms of their isolation from contaminating bacterial proteins during purification. These purification strategies involve the recovery of IBs from the insoluble fraction of the bacterial lysate and subsequent solubilization of isolated inclusion bodies using strong denaturants like urea, guanidine hydrochloride, or trifluoroethanol [27–29]. Such stringent denaturants influence both the physical and chemical properties of recombinant protein preparations produced with this approach. Additionally, the refolding of denatured proteins often does not reach completion once the denaturant is removed, thereby compromising the effective use of these eukaryotic proteins in their native functional state [30]. On a positive note, adding solubility tags or co-expressing recombinant proteins with molecular chaperones can significantly enhance their solubility [27,31,32].

Several solubility tags have been used to improve the solubility of hydrophobic or aggregation-prone polypeptides to ensure the recovery of expressed recombinant proteins in the lysate supernatant during purification [33]. Small Ubiquitin-like modifier (SUMO) protein, Maltose-binding protein (MBP), and Glutathione-S-transferase (GST) are the three most used tags to increase the solubility of fused proteins of interest produced in bacterial expression systems [34–36]. These solubility tags are sometimes used to aid in the purification of the fusion protein or even in downstream applications such as pull-down experiments or antibody-based detection of the tagged protein. However, in most cases, solubility tags are separated from the protein of interest via targeted proteolytic cleavage

of a specific recognition site placed between the tag and the protein-coding sequence [37]. Tobacco etch virus (TEV) protease, Thrombin, and SUMO protease (Ulp1) are the three most used proteases in the cleavage of solubility and affinity tags from the purified protein of interest [38–40]. A prime example of where a solubility tag played a pivotal role in improving the solubility of IDPs, including full-length Tau and some of its domain constructs, is our newly developed tandem-tag system (6xHis-SUMO-Tau-Heparin) [41]. Despite producing protein preparations of very high purity, the overall yield was limited for use in downstream applications like NMR titration experiments and biophysical protein–protein interaction studies. When Tau proteins are needed in such large quantities, their purification strategy usually involves a boiling step [42], as Tau can survive this harsh treatment because it is an IDP. However, boiling introduces adverse effects such as oxidation and deamination to the sample quality, compromising the use of such preparations in downstream applications involving protein–protein interactions.

The major ampullate spidroin-derived solubility tag (MaSp-NT*), inspired by how spiders produce silk proteins at high concentrations via the sequestration of their aggregation-prone regions in micelle-like structures [14], presents exciting avenues for producing large quantities of aggregation-prone proteins. The MaSp-NT* tag has been successfully used to boost the recombinant expression of aggregation-prone proteins and peptides [43,44], improving expression levels up to 40 fold [45]. To explore the applicability to Tau proteins, we designed MaSp-Tau constructs with a 6xHis tag at the N-terminus of the NT* solubility tag and a TEV cleavage site between the solubility tag and the Tau protein of interest (6xHis-NT*-TEV-Tau). This architecture ensured the formation of micelle-like particles in the bacterial cytosol to shield aggregation-prone regions of Tau proteins but also facilitated the purification of MaSp-Tau proteins in two simple purification steps before and after targeted proteolytic cleavage.

Here, we describe the use of MaSp-NT* solubility tag for the efficient expression and purification of wild-type Tau-hT40 and two of its variants (FTD-associated disease mutant; Tau-P301L and aggregation-prone microtubule-binding region; Tau-MTBR), which might otherwise be difficult to produce at high levels through recombinant methods.

2. Materials and Methods

2.1. Generation of pT7NT (MaSp) Tau Constructs*

2.1.1. Generating MaSp-Tau-hT40 Plasmid

The MaSp-Tau-hT40 expression plasmid (Supplementary Figure S3) was generated via modification of an existing one (pT7NT*-Aβ42, a gift from Dr. Henrik Biverstal, Karolinska Institutet; derived from parent plasmid, pT7NT*-Bri2 113–231 R221E, Addgene plasmid #138134; https://www.addgene.org/138134/, accessed on 9 February 2023) [14,46]. The pT7NT*-Aβ42 plasmid housed an N-terminal 6x His-tag followed by the NT* tag and the coding sequence for Amyloid beta-42 (Aβ42) protein in its multiple cloning site (MCS) under T7 promoter elements (Supplementary Figure S1). Following the manufacturer's instructions, this plasmid was used as a backbone vector to replace the Aβ42 coding sequence with a gene coding for full-length Tau-hT40 using the HiFi DNA Assembly Cloning kit (New England Biolabs (NEB), Ipswich, MA, USA) with Tau441-MaSp_F and Tau441-MaSp_R primers (Supplementary Table S1). The Tau-hT40-coding DNA fragment was amplified by the polymerase chain reaction (PCR) using the Q5 High-Fidelity DNA polymerase (NEB, Ipswich, MA, USA) kit, with an in-house Tau-hT40-containing plasmid as a template.

After successfully replacing the Aβ42 gene in the MaSp plasmid with the gene coding for Tau-hT40 (Supplementary Figure S2), a TEV cleavage site was inserted between the NT* tag and the Tau-hT40 coding sequence. This was achieved by site-directed mutagenesis (SDM) PCR using the High-Fidelity DNA polymerase kit with Tau441-TEV-MaSp_F and Tau441-TEV-MaSp_R primers (Supplementary Table S1). Unfortunately, the inserted TEV cleavage site was missing a T-nucleotide, resulting in a frame-shift mutation. This was corrected by additional SDM PCR using TFT_insTGGG_F and TFT_insTGGG_R primers

(Supplementary Table S1) that inserted a T-nucleotide and three additional G-nucleotides coding for the amino acid Glycine. Following mutagenesis PCR, modified plasmid DNA was used to transform NEB 5-alpha Competent *E. coli* cells (NEB5α). Luria Bertani (LB) agar with 50 μg/mL Kanamycin antibiotic (Duchefa Biochemie, Haarlem, The Netherlands) was used to select successful transformants. The resulting colonies were inoculated and propagated in LB liquid media to which 50 μg/mL Kanamycin antibiotic was added (LB-Kan). The MN-Nucleospin Plasmid QuickPure kit (Fisher Scientific, Merelbeke, Belgium) was employed to extract plasmids from the liquid cultures, according to the manufacturer's instructions. Before its use in recombinant protein expression, the MaSp-Tau-hT40 plasmid DNA sequence was verified by Sanger sequencing (Supplementary Figure S4), which was carried out at a Microsynth sequencing facility in Gottingen, Germany.

2.1.2. Generating MaSp-Tau-P301L Plasmid

The MaSp-Tau-P301L plasmid (Supplementary Figure S5) was generated by a single amino-acid substitution of Proline-301 in MaSp-Tau-hT40 to a Leucine via site-directed mutagenesis. The SDM PCR was carried out using the NEB Q5 High-Fidelity DNA polymerase kit with primers MaSp_P301L_F and MaSp_P301L_R (Supplementary Table S1). Treatment of the PCR products with a Kinase, Ligase, and DpnI (KLD) from NEB (Ipswich, MA, USA) ensured enrichment of nascent plasmid DNA housing the P301L mutation. LB-Kan agar plates were then used to select for transformants of NEB5α, and the MaSp-Tau-P301L plasmid sequences were confirmed by Sanger sequencing (Supplementary Figure S6) before their use in recombinant protein expression.

2.1.3. Generating MaSp-Tau-MTBR Plasmid

The MaSp-Tau-MTBR plasmid (Supplementary Figure S7) was generated similarly to MaSp-Tau-hT40 with minor modifications. The NEB HiFi DNA Assembly kit was used to replace the Aβ42 gene in the pT7NT*-Aβ42 plasmid with the coding sequence for Tau-MTBR (residues 225–372 of the full-length Tau441) using MTBR-MaSp_F and MTBR-MaSp_R primers (Supplementary Table S1). The template DNA employed in amplifying the Tau-MTBR coding sequence was a kind gift from Prof. Nicholas Kanaan at the Department of Translational Neuroscience, Michigan State University. Site-directed mutagenesis was used to insert a TEV cleavage site between the NT*tag and Tau-MTBR coding sequence using MTBR-MaSp+TEV_F and MTBR-MaSp+TEV_R primers (Supplementary Table S1). LB-Kan agar plates were employed to select NEB5α transformants, and the MaSp-Tau-MTBR sequence was confirmed by Sanger sequencing (Supplementary Figure S8) following single-colony propagation in LB-Kan liquid media and plasmid extraction, as described in the previous section.

2.2. Expression and Purification of MaSp-Tau Recombinant Proteins

2.2.1. Expression and Purification of MaSp-Tau-hT40

As the MaSp-Tau-hT40 construct was generated from plasmids that were codon-optimized for *E. coli* expression, recombinant protein production was carried out in *E. coli* BL21 Star™ (DE3) cells (NEB, Ipswich, MA, USA). Bacterial cells were cultured at 37 °C in Terrific broth (TB) that was prepared in-house and supplemented with 50 μg/mL of Kanamycin antibiotic. We induced expression by adding 1 mM isopropyl β-d-1-thiogalactopyranoside (IPTG) (Sigma-Aldrich, St. Louis, MO, USA) at OD_{600} = 1.2, and continued to culture cells for five hours at 30 °C while shaking at 180 rpm. Centrifugation of the bacterial culture at 4500 revolutions per minute (rpm) for 20 min using the Avanti JXN-26 (Beckman Coulter, CA, USA) pelleted the cells prior to their storage at −80 °C.

The purification of MaSp-Tau-hT40 started with resuspending a one-liter bacterial pellet in 100 mL of lysis buffer (50 mM HEPES (Sigma-Aldrich, St. Louis, MO, USA), 1 M NaCl (Sigma-Aldrich, St. Louis, MO, USA), 10 mM $MgCl_2$ (Merck, Darmstadt, Germany), 25 mM Imidazole (Merck, Darmstadt, Germany), 10% Glycerol (VWR, Solon, OH, USA), 0.1% Triton X-100 (Sigma-Aldrich, St. Louis, MO, USA), 1 μg/mL RNase A (ThermoFisher

Scientific, Waltham, MA, USA), 0.5 mM tris(2-carboxyethyl)phosphine (TCEP) (VWR, Solon, OH, USA), 1 mM phenyl-methyl-sulfonyl fluoride (PMSF) (Sigma-Aldrich, St. Louis, MO, USA), 1 mM Benzamidine hydrochloride (Sigma-Aldrich, St. Louis, MO, USA), and 2 of Roche complete protease inhibitor cocktail tablets (Merck, Darmstadt, Germany), pH 7.2) using a 50 mL glass homogenizer (Carl Roth, Karlsruhe, Germany). Resuspended cells were then lysed by sonication (5 s on/5 s off, 60% amplitude, 10 min, 4 °C), and the resulting bacterial lysate was centrifuged for 1 h at 40,000× *g* (4 °C) in the presence of 1 mg/mL DNase I (Sigma-Aldrich, St. Louis, MO, USA). The lysate supernatant was filtered using a 0.45 µm syringe filter (Sarstedt, Numbrecht, Germany), and every step was carefully performed on ice.

An ÄKTA Pure Protein Purification System housed in a cooling cabinet (GE Healthcare, Uppsala, Sweden) was used to load the filtered lysate onto two HisTrap-HP-5 mL columns (Cytiva, Uppsala, Sweden). The HisTrap binding buffer (A) was 50 mM HEPES, 1 M NaCl, 25 mM Imidazole, 1 mM TCEP, pH 7.2. After sample loading, buffer-A was applied to the columns to wash away bacterial chaperones and other contaminants that co-purify with Tau recombinant proteins. Bound proteins were eluted from the column by applying a gradient of elution buffer (B) composed of 50 mM HEPES, 1 M NaCl, 500 mM Imidazole, 1 mM TCEP, pH 7.2. Sodium dodecyl-sulfate polyacrylamide gel electrophoresis (SDS-PAGE) was employed to analyze the eluates, and fractions containing our protein of interest were pooled together in a sterile 50 mL Falcon tube (Greiner Bio-One, Vilvoorde, Belgium). Recombinant TEV protease enzyme was added to the HisTrap pool (0.15 mg/mL from a 5 mg/mL stock that was expressed and purified in-house) to cleave the N-terminal 6xHis-NT* tag. The protein mixture was immediately transferred to a 12–14 kDa MWCO dialysis membrane (Serva, Heidelberg, Germany) and dialyzed overnight against HisTrap buffer A in a cold room (4 °C).

The following morning, the TEV-digested protein mixture was recovered from the dialysis bag, placed into a fresh Falcon tube, and loaded onto two HisTrap-HP-5 mL columns equilibrated with HisTrap binding buffer A. In this Reverse HisTrap purification step, the cleaved 6xHis-NT* tag and TEV protease enzyme (housed a 6xHis-tag at its N-terminus) were retained onto the column, as the cleaved Tau-hT40 was recovered in the HisTrap flow-through and wash fractions. Further purification steps (including anion exchange, cation exchange, and size-exclusion chromatography) did not improve the purity of the cleaved Tau-hT40 final product. The Reverse HisTrap flow-through and wash fractions were pooled together and dialyzed against Storage buffer (25 mM HEPES, 1M NaCl, 10% Glycerol, and 1mM TCEP) using a 12–14 kDa MWCO dialysis membrane. Ultrafiltration with a 10 kDa MWCO VivaSpin centrifugal filter (Sartorius, UK) was employed to concentrate the dialyzed sample, after which the protein concentration was determined by measuring absorbance at 280 nm (Tau-hT40 molecular weight—45.937 kDa; extinction coefficient—7450) using NanoDrop^{TM}One (ThermoFisher Scientific, Waltham, MA, USA). Purified Tau-hT40 was aliquoted, snap-frozen in liquid nitrogen, and immediately stored at −80 °C. The final yield from one liter of bacterial culture was 25 mg of Tau-hT40 purified protein.

2.2.2. Expression and Purification of MaSp-Tau-P301L

The MaSp-Tau-P301L construct was also produced in *E. coli* BL21 Star™ (DE3) cells, considering it was a product of MaSp-Tau-hT40 mutagenesis, which was already codon optimized for bacterial recombinant expression. Bacterial cells were cultured at 37 °C in TB growth media containing 50 µg/mL of Kanamycin antibiotic until an OD_{600} = 1.2 was attained. However, since this FTD-associated mutant version of Tau had a higher propensity to aggregate than the wild type, the recombinant protein was expressed at 20 °C overnight with relatively slow shaking (150 rpm) after induction by 1 mM IPTG. This ensured a slower expression of the MaSp-Tau-P301L to allow time for NT*tag-associated micelle-like particles to form and sequester aggregation-prone Tau-P301L polypeptides as they were being produced by bacterial ribosomes [14].

The purification strategy for MaSp-Tau-P301L followed a similar workflow to that of MaSp-Tau-hT40 with minor modifications. Bacterial lysate from a one-liter pellet was prepared and loaded onto two HisTrap-HP-5 mL columns equilibrated with HisTrap binding buffer A (containing 250 mM NaCl instead of 1 M). Following a washing step with the same buffer, bound proteins were eluted with HisTrap buffer B, which contained a higher concentration of Imidazole. Eluates containing MaSp-Tau-P301L were pooled and dialyzed against HisTrap buffer A in the presence of 0.15 mg/mL of TEV protease enzyme to cleave Tau-P301L from the 6xHis-NT* tag. Purified Tau-P301L was separated from cleaved NT*tag and TEV protease enzyme via a Reverse HisTrap purification step described above for MaSp-Tau-hT40.

Since the majority of cleaved Tau-P301L was recovered from the Reverse HisTrap elution fractions due to nucleic acid contamination, Cation exchange (CIEX) chromatography was employed to overcome this limitation and serve as a final polishing step. All Reverse HisTrap fractions containing cleaved Tau-P301L were pooled together and dialyzed for four hours against CIEX buffer A (25 mM MES buffer, 50 mM NaCl, 10% Glycerol, 1 mM TCEP, pH 5.5). The dialyzed protein mixture was then loaded onto a HiTrap-SP-5mL cation exchange column equilibrated with the same buffer. After a washing step with buffer A, bound proteins were eluted with a salt gradient using CIEX buffer B (buffer A with 1 M NaCl instead of 50 mM NaCl). SDS-PAGE was used to analyze the eluates and fractions containing purified Tau-P301L were concentrated as described above. By measuring absorbance at 280 nm (Tau-P301L molecular weight—45.953 kDa; extinction coefficient—7450), the protein concentration of the final preparation was determined. Purified Tau-P301L was aliquoted, snap-frozen in liquid nitrogen, and immediately stored at −80 °C. The final yield from one liter of bacterial culture was 29 mg of Tau-P301L-purified protein.

2.2.3. Expression and Purification of MaSp-Tau-MTBR

The MaSp-Tau-MTBR construct was also produced at high levels in *E. coli* BL21 Star™ (DE3) cells, considering it was assembled from plasmids that were codon optimized for bacterial recombinant expression. This shorter Tau domain was expressed and purified the same way as MaSp-Tau-hT40 with additional modifications to account for its aggregation-prone nature. Similar to our observations with other in-house Tau-MTBR plasmids, expressing MaSp-Tau-MTBR for five hours at 30 °C resulted in the sequestration of a fraction of the recombinant protein in bacterial inclusion bodies. The slow expression strategy of MaSp-Tau-MTBR substantially improved the protein's recovery in the supernatant of the bacterial lysate. This strategy entailed using a lower concentration of the inducer (0.5 mM IPTG) and culturing the cells for 20 h at 16 °C with slow shaking (120 rpm).

MaSp-Tau-MTBR purification involved an additional polishing step (size-exclusion chromatography; SEC) after the HisTrap and Reverse HisTrap purification steps described for MaSp-Tau-hT40 above. Unlike MaSp-Tau-hT40 and MaSp-Tau-P301L, taking the Reverse HisTrap Pool sample through SEC succeeded in separating cleaved Tau-MTBR from its two dominant degradation fragments and the bacterial chaperone DnaK (Hsp70) that co-purifies with this construct. SEC was performed using the Superdex 75 (16/600) column equilibrated with Storage buffer at a constant 1 mL/min flow rate. Isocratically eluted fractions containing pure Tau-MTBR were concentrated by ultrafiltration using the 5 kDa MWCO centrifugal concentrators (Sartorius, Stonehouse, UK). The protein sample was then aliquoted, snap-frozen in liquid nitrogen, and stored at −80 °C. The final yield of purified Tau-MTBR was 41 mg from 1 L of bacterial culture.

2.3. Nuclear Magnetic Resonance (NMR) Spectroscopy

The NMR sample contained 0.4 mM U-[^{13}C, ^{15}N] Tau-MTBR in 20 mM Tris-HCl pH 6.5, 100 mM NaCl, and 6% D_2O for the lock. All NMR spectra were acquired at 298 K on a Bruker Avance III HD 800 MHz spectrometer equipped with a TCI cryoprobe for enhanced sensitivity. The experimental set comprised 2D [^{1}H, ^{15}N] HSQC and 3D BEST-HNCACB, BEST-HN(CO)CACB, BEST-HNCO, and BEST-HN(CA)CO spectra. All 3D experiments

were acquired with a non-uniform sampling (20–50%) as implemented in TopSpin 3.6 (Bruker). The NMR data were processed in TopSpin 3.6 (Bruker) or MddNMR [47] and NMRPipe [48], and analyzed in CCPNMR [49]. The assignments of N, NH, Hα, Hβ, CO, Cα, and Cβ atoms were obtained from the identification of intra- and inter-residue connectivities in HNCACB, HN(CO)CACB, HNCO, and HN(CA)CO spectra at the ^{1}H,^{15}N frequencies of every peak in the HSQC spectrum. The ^{1}H, ^{13}C, and ^{15}N chemical shifts for backbone atoms of Tau-MTBR have been deposited in the Biological Magnetic Resonance Bank (BMRB) under the accession number 52503.

3. Results

3.1. MaSp (NT) Plasmids Designed for Improved Expression of Tau Constructs*

Generally, most expression plasmids designed for challenging and aggregation-prone proteins have a solubility tag at one or both termini to improve the solubility of the recombinant protein fusion as it accumulates in the cytosol of bacterial cells [45,50]. Such solubility tags usually house an affinity tag that aids in the first purification step of the fusion protein. The solubility tag is then separated from the protein of interest via enzymatic cleavage of a specific recognition sequence inserted between the solubility tag and the protein of interest. The two would then be separated by a reverse affinity purification step where the protein of interest is recovered in the flow-through fraction as the solubility tag is retained on the column [51]. The spidroin-derived solubility tag (NT* tag), however, not only improves the solubility of aggregation-prone polypeptides but also dramatically enhances the expression level of the fusion protein [14]. This enabled the production and purification of difficult Tau constructs at high yields without a boiling step.

The MaSp-Tau constructs were designed purposefully to improve both the solubility and yield of aggregation-prone Tau proteins. We generated MaSp-Tau plasmids for bacterial expression (under the control of a strong T7 promoter) from an existing plasmid designed to improve the expression of another aggregation-prone protein, Aβ42. MaSp-Tau constructs had a 6xHis-tag conjugated to the NT* solubility tag on the N-terminus. The NT* tag facilitated high-level expression and improved the solubility of the Tau proteins but did not participate in affinity purification, hence the need for a 6xHis-tag to drive HisTrap purification of recombinant proteins. TEV protease cleavage sites were inserted between the NT* tag and Tau protein-coding sequences to enable the separation of Tau recombinant proteins from the 6xHis-NT* tag during purification (Figure 1A). The effectiveness of this production and purification strategy was demonstrated using wild-type Tau protein (Tau-hT40), its FTD-associated mutant variant (Tau-P301L), and the aggregation-prone microtubule-binding region (Tau-MTBR) (Figure 1B).

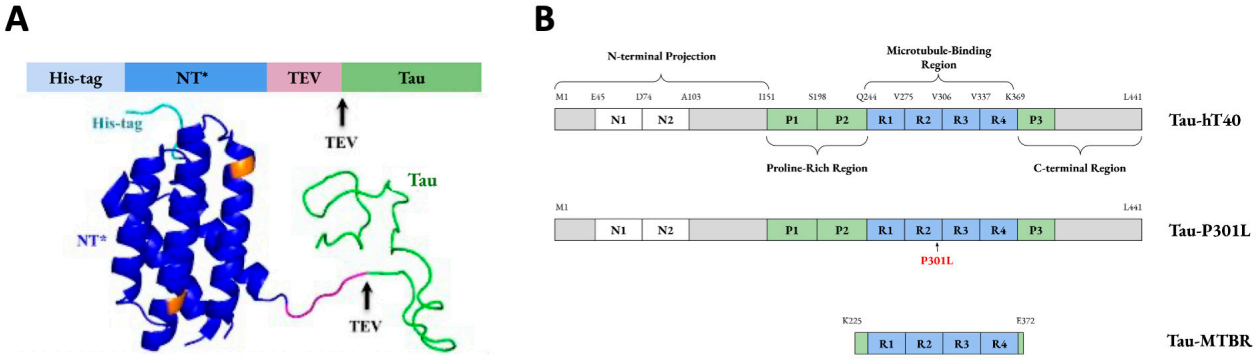


Figure 1. (**A**) Schematic representation of MaSp-Tau constructs housing a 6xHis-NT* tag at the N-terminus and the Tau protein of interest at the C-terminus separated by a TEV cleavage site. The black arrows indicate the TEV protease cleavage site in the TEV recognition sequence [ENLYFQ|S]. The figure was adapted from [44]. (**B**) Domain architecture of the three Tau proteins produced and purified using MaSp-Tau plasmids.

3.2. Expression and Purification of NT Tau Recombinant Proteins*

3.2.1. Expression and Purification of MaSp-Tau-hT40

Tau is a microtubule-associated protein aggregated in several neurodegenerative disorders, collectively referred to as tauopathies [52]. The most common tauopathies are AD and FTD, where different Tau isoforms aggregate as NFTs or amorphous inclusions, respectively, in affected neuronal cells [8]. In the physiological context, six distinct Tau isoforms are generated through alternative splicing of the precursor messenger RNA (pre-mRNA) transcribed from the MAPT gene [53]. The isoforms exhibit variability in the number of N-terminal inserts (N1, N2) and imperfect repeats (R1–R4, constituting its microtubule-binding region, MTBR) in their C-terminal half. The shortest isoform found in the adult human brain has 352 amino acid residues (0N3R), while the longest isoform has 441 residues (2N4R or Tau441 or ht40) [54]. The liquid–liquid phase separation of Tau-hT40 has recently been implicated in fostering its pathological aggregation and has sparked the need for more scientific research in both academic and industrial settings. However, since it behaves as an IDP in solution, Tau-hT40 is studied using solution-based structural techniques such as NMR spectroscopy and SAXS. These techniques often require recombinant protein preparations of high purity and yield, which are not readily produced and purified from bacteria without encountering challenges presented by bacterial inclusion bodies and boiling the bacterial lysate during purification [55]. To circumvent these challenges, we employed the NT* solubility tag to enhance the expression and solubility of the Tau-hT40 recombinant protein.

Recombinant production of Tau-hT40 using the NT* tag substantially enhanced its expression levels and solubility, which in turn improved the yield of NT* Tau-hT40 fusion recovered in the soluble fraction of the bacterial lysate without the need for boiling or solubilization of inclusion bodies (Figure 2). This recovery was evidenced by the fact that MaSp-Tau-hT40 from 1 L of pellets completely saturated a HisTrap-HP-5mL column and required the combination of two such columns to avoid spillage of the recombinant protein in the HisTrap flow-through during sample loading (Figure 2). A one-liter bacterial pellet of MaSp-Tau-hT40 was resuspended in standard lysis buffer supplemented with several protease inhibitors. Growing bacteria in the richer TB media instead of LB media comes with the advantage of producing a higher cell density in the same volume of culture before inducing recombinant protein expression with the addition of IPTG. However, bacterial lysates from cells cultured in TB growth media also produce relatively larger amounts of messenger RNA [56] that co-purify with charged and sticky IDPs like Tau. This explains why RNase A was incorporated into the lysis buffer. Additionally, the NaCl concentration in the lysis buffer was increased by up to one molar to further counter the nucleic acid contamination as well as the levels of bacterial Hsp70 (DnaK) that often elute with Tau proteins during HisTrap purification [57].

The purification of MaSp-Tau-hT40 followed standard immobilized metal-affinity chromatography using Ni^{2+}-charged columns and standard buffers (Binding buffer with low Imidazole and Elution buffer with high Imidazole). Following bacterial cell lysis, the lysate supernatant was loaded onto two HisTrap columns, which enriched the target protein via the 6xHis tag, as untagged bacterial proteins were washed away (Supplementary Figure S9). Elution fractions that contained MaSp-Tau-hT40 were pooled together and supplemented with purified recombinant TEV protease enzyme. Targeted proteolytic cleavage by TEV protease to separate Tau-hT40 from the NT* solubility tag was performed in HisTrap buffer A while dialyzing the protein mixture at 4 °C overnight. This setup allowed ample time for the TEV protease to achieve maximal cleavage while buffer exchanging the protein sample to reduce the Imidazole concentration in preparation for Reverse HisTrap purification. This purification step served to separate the cleaved Tau-hT40 from the uncleaved MaSp-Tau-hT40 fusion protein, the cleaved NT* tag, and the TEV protease enzyme that housed a 6xHis-tag at its N-terminus. Purified Tau-hT40 was collected from the Reverse HisTrap Wash fraction as the other components were recovered in elution fractions (Figure 2 and Figure S10). The final product was relatively pure, with some Tau-hT40 degradation

fragments and dimers that could not be eliminated with further purification steps (ion exchange or SEC).

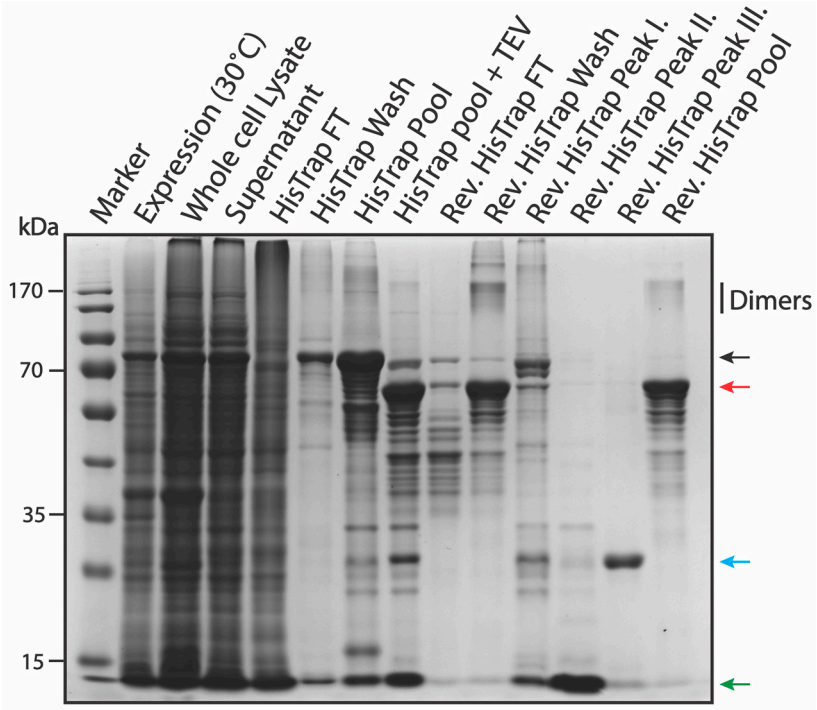


Figure 2. SDS-PAGE gel summarizing the purification of MaSp-Tau-hT40. The black arrow indicates the MaSp-Tau-hT40 fusion protein, the red arrow indicates the cleaved final product, the green arrow indicates the cleaved NT* tag and the blue arrow indicates the TEV protease enzyme eluted from the column during the Reverse HisTrap purification step. Tau-hT40 dimers (16.4%) in the final product are also displayed on the gel image.

3.2.2. Expression and Purification of MaSp-Tau-P301L

In Tau protein, the P301L mutation is the most prevalent and it is linked to neurodegenerative frontotemporal dementia, accounting for approximately 10–20% of FTD cases worldwide [58]. This mutation has recently been reported only to potentiate but not sufficient to cause the formation of cytotoxic Tau fibrils [59]. The Proline to Leucine amino acid substitution results in a polypeptide chain with relatively higher hydrophobicity and propensity to aggregate when compared to the wild-type protein. This change is also reflected in the protein produced recombinantly using different expression systems. Therefore, extra precautions must be taken to ensure the expressed protein is not sequestered in bacterial inclusion bodies. The NT* solubility tag was designed to curb such limitations during the recombinant production of aggregation-prone proteins using a bacterial expression system.

The MaSp-Tau-P301L expression and purification workflows were similar to those described for MaSp-Tau-hT40 with minor modifications. Recombinant protein expression was carried out in TB growth media, and purification started with resuspending a 1 L bacterial pellet in lysis buffer supplemented with protease inhibitors. This lysis buffer was not supplemented with RNase A and only had 0.25 M NaCl instead of 1 M NaCl. Under these conditions, excessive nucleic acid and DnaK contamination were observed in the HisTrap elution fractions that also contained MaSp-Tau-P301L (Supplementary Figure S11). The nucleic acid contamination caused turbidity in the dialysis bag as TEV protease cleaved the NT* solubility tag from Tau-P301L. The turbidity could be cleared by adding more salt to the protein mixture. Interestingly, the majority of cleaved Tau-P301L was recovered from elution fractions instead of the flow-through and wash fractions of the Reverse HisTrap purification step (Supplementary Figure S12). This observation could

also be attributed to the nucleic acid contamination that hindered the passage of cleaved Tau-P301L through the column due to charge interactions. An additional purification step (Cation exchange chromatography; CIEX) was required to separate purified Tau-P301L from nucleic acid contaminants (A260/A280 ratio = 0.56), considering the fact that the cation exchanger was negatively charged and was not a favorable interaction surface for nucleic acids (Supplementary Figure S13). These observations prompted adjustments—like increasing the salt concentration and adding RNase A in the lysis buffer—that were made during the purification of Tau-hT40 and Tau-MTBR. Notably, cation exchange (Figure 3) and other chromatographic separation steps (anion exchange and SEC) did not substantially improve the purity of the final product, as observed during the purification of Tau-hT40.

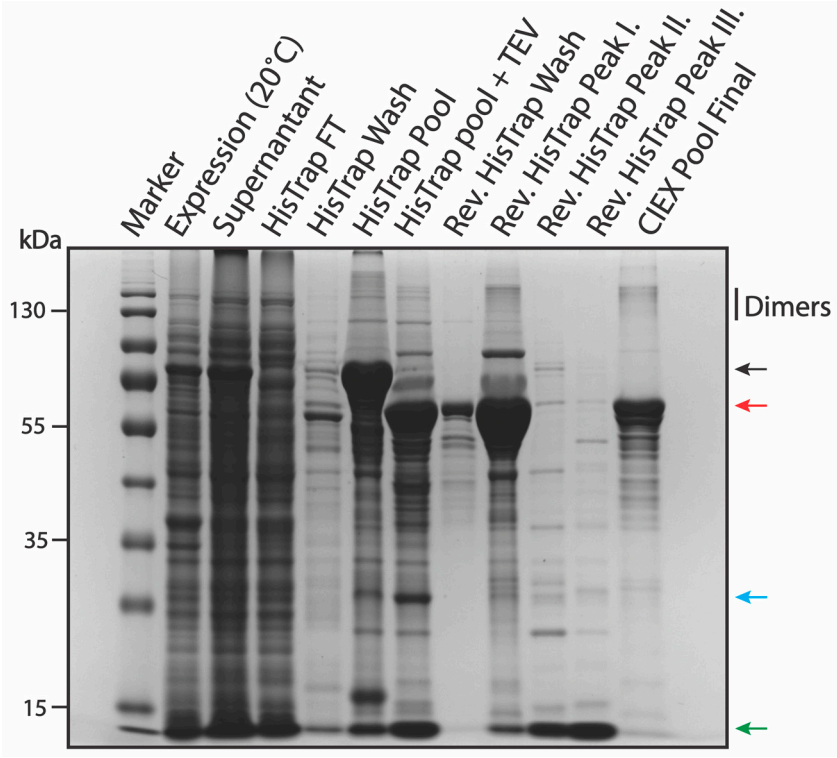


Figure 3. SDS-PAGE gel summarizing the purification of MaSp-Tau-P301L. The black arrow indicates the MaSp-Tau-P301L fusion protein, the red arrow indicates the cleaved final product, the green arrow indicates the cleaved NT* tag, and the blue arrow indicates the TEV protease enzyme eluted from the column during the Reverse HisTrap purification step. Tau-P301L dimers (14.3%) in the final product are also displayed on the gel image.

3.2.3. Expression and Purification of MaSp-Tau-MTBR

The complexity of Tau biology extends beyond its recognized involvement in microtubule polymerization and cytoskeleton structure stabilization to crucial functional roles in regulating axonal transport. In the physiological context, Tau predominantly resides in neuronal axons, where its microtubule-binding domain (Tau-MTBR) mediates tubulin interactions, fostering microtubule assembly, stability, and spacing [60–63]. Meanwhile, the phase separation of Tau to orchestrate the formation of membraneless organelles further underscores the protein's versatile nature, providing critical insights into the complex mechanisms contributing to tauopathies. Tau-MTBR is central to the formation of amyloid and amorphous aggregates in various tauopathies. It houses two crucial hydrophobic hexapeptide motifs, which are essential for both the seeding and propagation of Tau aggregates [64,65]. Moreover, the aggregation propensity of Tau is also influenced by the oxidation state of its two native cysteine residues (Cys291 and Cys322) [66], which reside in this repeat domain. Tau-MTBR does not undergo liquid–liquid phase separation in isolation, even under crowding conditions [6]. However, various studies have reported its

complex coacervation with polyanions and other chemical compounds with a high negative charge [4,67,68]. This evolving comprehension of Tau's multifaceted roles, intertwining LLPS and aggregation dynamics, holds the potential to unravel the pathogenic mechanisms of tauopathies and unveil novel therapeutic avenues.

The MaSp-Tau-MTBR expression and purification workflows were also like those described for MaSp-Tau-hT40 with minor modifications. Compared to other in-house expression constructs for this highly hydrophobic and aggregation-prone Tau domain, the presence of the spidroin-derived NT* tag substantially enhanced its expression as well as its recovery in the lysate supernatant (Figure 4). The MaSp-Tau-MTBR slow expression (0.5 mM IPTG, 20 h, 16 °C, 120 rpm) delivered very high expression levels, which estimated to be magnitudes of up to 20 times higher when compared to those expressing other aggregation-prone proteins under identical conditions (Supplementary Figure S14). As described before, HisTrap purification enriched MaSp-Tau-MTBR at the expense of contaminating bacterial proteins (Supplementary Figure S15). Based on the lessons learned during the purification of Tau-P301L, the lysis buffer was supplemented with high levels of salt and RNase A to limit the disturbances caused by nucleic acid contamination. Indeed, no turbidity was observed in the dialysis bag during the TEV-mediated proteolytic cleavage. Additional TEV (0.25 mg/mL) to the HisTrap pool ensured complete digestion of MaSp-Tau-MTBR fusion protein to recover as much of the cleaved final product in the wash fraction of the Reverse HisTrap purification step (Supplementary Figure S16). Finally, the adjustment of adding 1 M NaCl in the lysis buffer and HisTrap buffers did not completely abolish the DnaK contamination from cleaved Tau-MTBR in the Reverse HisTrap Wash fraction (Figure 4). Adding 10 mM TCEP and subjecting the protein mixture to size-exclusion chromatography separated purified Tau-MTBR from DnaK and the two most dominant degradation fragments (Supplementary Figure S17).

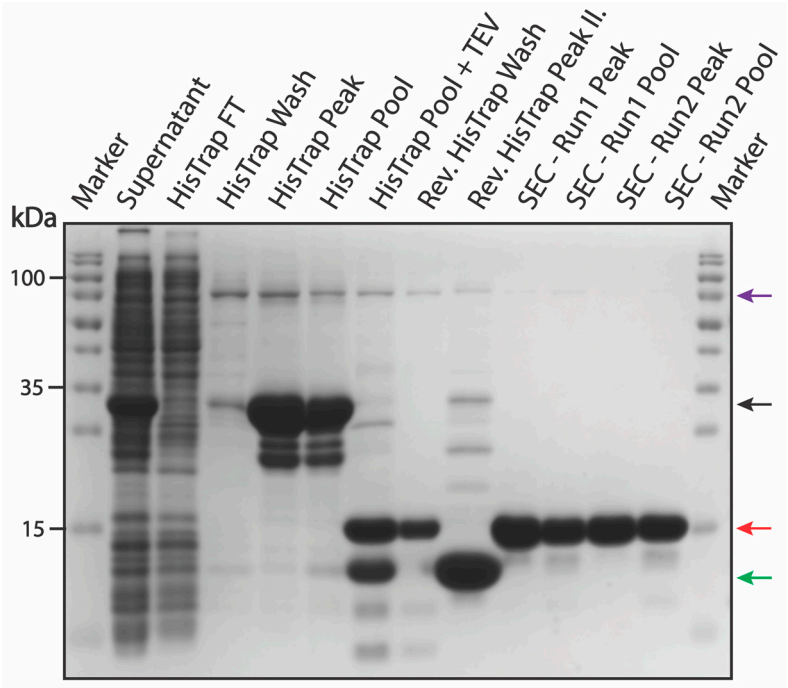


Figure 4. SDS-PAGE gel summarizing the purification of MaSp-Tau-MTBR. The black arrow indicates the MaSp-Tau-MTBR fusion protein, the red arrow indicates the cleaved final product, the green arrow indicates the cleaved NT* tag, and the purple arrow indicates the DnaK (bacterial Hsp70) contaminant.

3.3. Characterization of Purified Tau-MTBR by Solution NMR Spectroscopy

The expression of the Tau-MTBR construct in a minimal medium supplemented with $^{15}NH_4Cl$ and ^{13}C-labeled glucose as the sole nitrogen and carbon sources, respectively, allows for the preparation of a uniformly [^{13}C, ^{15}N]-labeled protein suitable for biomolecular

NMR spectroscopy. The isotopically labeled Tau-MTBR sample exhibits a well-resolved [^{1}H, ^{15}N] heteronuclear single quantum correlation (HSQC) spectrum (Figure 5), with the correct number of resonances corresponding to the backbone amide NH groups and the absence of any minor signals testifying to the high purity of the protein. Thanks to the good quality of the Tau-MTBR sample and its favorable spectral properties, we have obtained near-complete assignments of the protein backbone atoms. Except for the C99 resonance (not observed in this work) and strongly overlapping signals of glycine residues in repetitive PGGG motifs (which could not be unambiguously assigned), we have established full assignments of NH, Cα, Cβ, and CO atoms of Tau-MTBR.

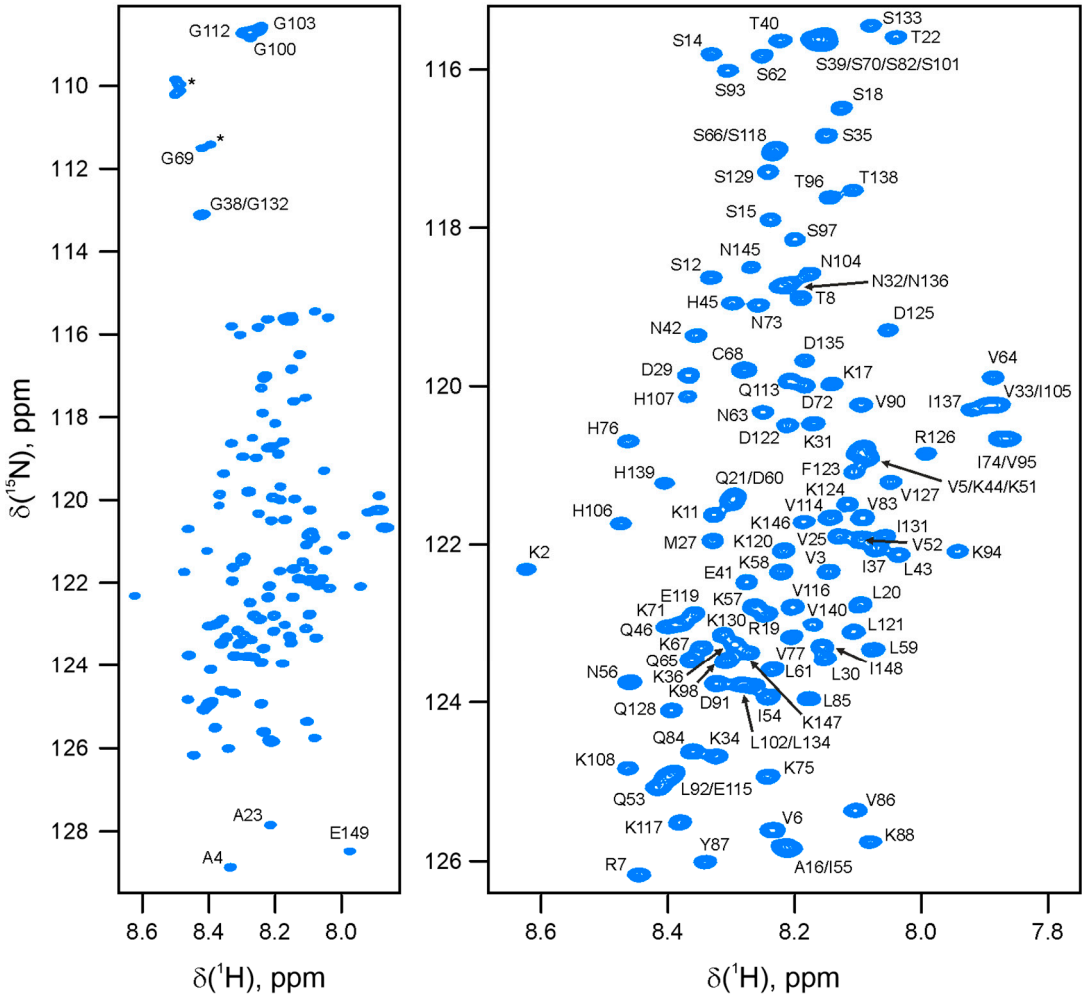


Figure 5. Assigned [^{1}H,^{15}N]-HSQC spectrum of purified Tau-MTBR. Full backbone amide region (**left**) and zoom in of the central part (**right**) annotated with the assignments of the Tau-MTBR backbone amides. The residues of the Tau-MTBR construct used for NMR experiments are labeled consecutively, starting from Lys-2 to Glu-149 (corresponding to Lys-225 and Glu-372 of the full-length Tau441). The asterisks indicate amide resonances of glycines in repetitive PGGG motifs, which could not be unambiguously assigned. The spectra were recorded in 20 mM Tris-HCl pH 6.5, 100 mM NaCl at 298 K.

The [^{1}H, ^{15}N]-HSQC spectrum of Tau-MTBR closely resembles that reported for the Tau-MTBR recombinant protein [69]. Small discrepancies in the exact positions of backbone amide resonances can be attributed to differences in the experimental conditions (20 mM Tris-HCl pH 6.5, 100 mM NaCl and 298 K in this work, versus 20 mM sodium phosphate pH 7.4, 100 mM NaCl and 283 K in [69]). The high similarity of the HSQC spectra of the two constructs indicates that the expression/purification strategy presented here does

not impair the structural integrity and has no impact on the biophysical properties of the recombinant protein.

4. Discussion

Improving the expression and purification of aggregation-prone IDPs produced recombinantly remains a challenge. Because of their unique properties, these proteins are often difficult to purify. Owing to their significant roles in phase separation, aggregation, and other cellular processes, they are highly sought after but require preparations of high quantity and purity for use in laboratory experiments. This article outlines a way to overcome low yields of aggregation-prone recombinant proteins by using a bio-inspired solubility tag that can boost yields up to twenty-fold. The approach involved using the major ampullate spidroin-derived solubility tag (MaSp-NT*), which shows that the NT* tag not only improves the solubility of Tau constructs but also significantly boosts their production, addressing a crucial bottleneck in tauopathy research. The three Tau variants tested—full-length Tau (hT40/Tau441), the FTD-associated mutant (Tau-P301L), and the highly aggregation-prone microtubule-binding repeat domain (Tau-MTBR)—all benefited from the use of the NT* tag, demonstrating the robustness of the solubility tag and the broad applicability of this method. The NT* tag's capacity to increase the solubility and yield of aggregation-prone proteins is particularly advantageous for Tau proteins, which are known to form insoluble aggregates [3,59].

Traditional purification strategies for Tau proteins often involve the use of harsh conditions, such as boiling [42] or solubilization from bacterial inclusion bodies [29], thereby jeopardizing protein integrity and, in turn, the downstream applications of the purified protein. The NT* tag works around this by stimulating the formation of micelle-like structures that sequester hydrophobic and aggregation-prone regions, thereby enhancing the solubility and overall yield of such stubborn proteins in the cytoplasm of *E. coli*. This approach streamlines the purifying process while preserving the protein's original structure, which is essential for downstream applications such as NMR or SAXS, which require large amounts of Tau protein to study its structure and protein–protein interactions. Solution NMR spectroscopy of Tau-MTBR demonstrated that the recombinant proteins produced and purified using this strategy were of high quality and not impaired in terms of their structural integrity or biophysical properties (Figure 5).

Other solubility tags have been used in the Tau field to improve the solubility of recombinant Tau proteins produced using a bacterial expression system [41,70]. However, the NT* solubility tag has the competitive advantage of enhancing the solubility of recombinant proteins with relatively low solubility and substantially boosting the overall yield of the purified protein. This spidroin-derived NT*tag presents a naturally occurring way of raising the solubility of aggregating proteins that is bio-inspired by how spiders accumulate such aggregation-prone polypeptides in their storage sacs until such a time when they are required as building blocks for spider-silk formation [14]. This method has been applied to three Tau proteins (Tau-hT40, Tau-P301L, and Tau-MTBR), each presenting unique challenges during the production and purification pipeline. Improved production of aggregation-prone variants of Tau protein opens new possibilities for further research into tauopathies' pathogenic processes, including Tau's participation in LLPS and its eventual progression to pathological aggregates.

In conclusion, the MaSp-NT* solubility tag represents an effective tool for producing and purifying aggregation-prone proteins such as Tau hydrophobic domains or mutant variants. Its ability to increase solubility and yield while maintaining protein integrity makes it an important tool for studying tauopathies and other IDP-related disorders. This approach makes it easier to produce high-quality recombinant proteins and opens new avenues for research into the molecular underpinnings of protein aggregation and its role in disease pathology. The IDP literature abounds with disease-linked proteins that are difficult to handle. Thus, the example of Tau proteins presented here may also inspire and boost studies related to other vital systems.

As a final note, further development of the NT* tagging method could focus on improving the purification technique to boost purity and eliminate possible contaminants such as nucleic acids. Furthermore, investigating the use of the NT* tag in eukaryotic expression systems may broaden its benefits to proteins that require post-translational modifications for full functionality. Comparative research with alternative solubility tags may also assist in determining the most successful approach for certain proteins or applications.

Supplementary Materials: The following supporting information can be downloaded at: https://www.mdpi.com/article/10.3390/separations11070198/s1, Table S1: List of primer sets used for HiFi cloning and site-directed mutagenesis; Figures S1–S8: Vector maps and sequencing results for MaSp-Tau plasmids; Figures S9–S17: SDS-PAGE gel images of MaSp-Tau constructs at various stages of purification.

Author Contributions: Conceptualization, K.M., G.R. and P.T.; Formal analysis, K.M. and A.V.; Funding acquisition, K.M., G.R. and P.T.; Investigation, K.M., B.Y., A.M. and A.V.; Methodology, K.M., A.M., G.R. and A.V.; Project administration, K.M. and P.T.; Supervision, K.M., A.M., G.R. and P.T.; Validation, K.M., A.M. and A.V.; Visualization, K.M., B.Y. and A.V.; Writing—original draft, K.M., B.Y. and P.T.; Writing—review and editing, K.M. and P.T. All authors have read and agreed to the published version of the manuscript.

Funding: This work was supported by grants K124670 and K131702 from the National Research, Development and Innovation Office (NKFIH, Hungary, to P.T.) and FWO PhD fellowships in fundamental research (11D0122N, to K.M.) and strategic basic research (FWOSB72, to G.R.).

Data Availability Statement: The data presented in this study are available on request from the corresponding author. The ^{1}H, ^{13}C and ^{15}N chemical shifts for backbone atoms of Tau-MTBR are available in BMRB [https://bmrb.io] under the accession number 52503.

Acknowledgments: The authors thank Henrik Biverstal and colleagues at the Karolinska Institutet for sharing the pT7NT*-Aβ42 plasmid from which other MaSp-Tau constructs were derived. The authors also thank Nicholas Kanaan and colleagues at Michigan State University for sharing the Tau plasmids from which Tau-hT40 and Tau-MTBR protein-coding sequences were obtained for cloning.

Conflicts of Interest: The authors declare no conflict of interest.

References

1. Yang, H.; Li, J.-Y.; Liu, J. *Protein Aggregation and Propagation in Neurodegenerative Diseases*; Frontiers: Lausanne, Switzerland, 2022; ISBN 9782832504765.
2. Chung, D.-E.C.; Roemer, S.; Petrucelli, L.; Dickson, D.W. Cellular and Pathological Heterogeneity of Primary Tauopathies. *Mol. Neurodegener.* **2021**, *16*, 57. [CrossRef]
3. Medeiros, R.; Baglietto-Vargas, D.; LaFerla, F.M. The Role of Tau in Alzheimer's Disease and Related Disorders. *CNS Neurosci. Ther.* **2011**, *17*, 514–524. [CrossRef]
4. Ambadipudi, S.; Biernat, J.; Riedel, D.; Mandelkow, E.; Zweckstetter, M. Liquid-Liquid Phase Separation of the Microtubule-Binding Repeats of the Alzheimer-Related Protein Tau. *Nat. Commun.* **2017**, *8*, 275. [CrossRef]
5. Wegmann, S.; Eftekharzadeh, B.; Tepper, K.; Zoltowska, K.M.; Bennett, R.E.; Dujardin, S.; Laskowski, P.R.; MacKenzie, D.; Kamath, T.; Commins, C.; et al. Tau Protein Liquid-Liquid Phase Separation Can Initiate Tau Aggregation. *EMBO J.* **2018**, *37*, e98049. [CrossRef]
6. Kanaan, N.M.; Hamel, C.; Grabinski, T.; Combs, B. Liquid-Liquid Phase Separation Induces Pathogenic Tau Conformations in Vitro. *Nat. Commun.* **2020**, *11*, 2809. [CrossRef]
7. Tompa, P. Intrinsically Disordered Proteins: A 10-Year Recap. *Trends Biochem. Sci.* **2012**, *37*, 509–516. [CrossRef]
8. Lee, G.; Leugers, C.J. Tau and Tauopathies. *Prog. Mol. Biol. Transl. Sci.* **2012**, *107*, 263–293. [CrossRef]
9. Schuler, B.; Soranno, A.; Hofmann, H.; Nettels, D. Single-Molecule FRET Spectroscopy and the Polymer Physics of Unfolded and Intrinsically Disordered Proteins. *Annu. Rev. Biophys.* **2016**, *45*, 207–231. [CrossRef]
10. Wingfield, P.T. Overview of the Purification of Recombinant Proteins. *Curr. Protoc. Protein Sci.* **2015**, *80*, 6.1.1–6.1.35. [CrossRef]
11. Walsh, G. Biopharmaceutical Benchmarks 2018. *Nat. Biotechnol.* **2018**, *36*, 1136–1145. [CrossRef]
12. Kim, Y.; Bigelow, L.; Borovilos, M.; Dementieva, I.; Duggan, E.; Eschenfeldt, W.; Hatzos, C.; Joachimiak, G.; Li, H.; Maltseva, N.; et al. Chapter 3. High-Throughput Protein Purification for X-Ray Crystallography and NMR. *Adv. Protein Chem. Struct. Biol.* **2008**, *75*, 85–105. [CrossRef] [PubMed]
13. Edwards, A.M.; Arrowsmith, C.H.; Christendat, D.; Dharamsi, A.; Friesen, J.D.; Greenblatt, J.F.; Vedadi, M. Protein Production: Feeding the Crystallographers and NMR Spectroscopists. *Nat. Struct. Biol.* **2000**, *7*, 970–972. [CrossRef] [PubMed]

14. Kronqvist, N.; Sarr, M.; Lindqvist, A.; Nordling, K.; Otikovs, M.; Venturi, L.; Pioselli, B.; Purhonen, P.; Landreh, M.; Biverstål, H.; et al. Efficient Protein Production Inspired by How Spiders Make Silk. *Nat. Commun.* **2017**, *8*, 15504. [CrossRef] [PubMed]
15. Schmidt, T.G.M.; Skerra, A. The Strep-Tag System for One-Step Purification and High-Affinity Detection or Capturing of Proteins. *Nat. Protoc.* **2007**, *2*, 1528–1535. [CrossRef] [PubMed]
16. Tripathi, N.K.; Shrivastava, A. Recent Developments in Bioprocessing of Recombinant Proteins: Expression Hosts and Process Development. *Front. Bioeng. Biotechnol.* **2019**, *7*, 420. [CrossRef] [PubMed]
17. Demain, A.L.; Vaishnav, P. Production of Recombinant Proteins by Microbes and Higher Organisms. *Biotechnol. Adv.* **2009**, *27*, 297–306. [CrossRef] [PubMed]
18. Adrio, J.-L.; Demain, A.L. Recombinant Organisms for Production of Industrial Products. *Bioeng. Bugs* **2010**, *1*, 116–131. [CrossRef] [PubMed]
19. Gupta, S.K.; Shukla, P. Advanced Technologies for Improved Expression of Recombinant Proteins in Bacteria: Perspectives and Applications. *Crit. Rev. Biotechnol.* **2016**, *36*, 1089–1098. [CrossRef] [PubMed]
20. Ferrer-Miralles, N.; Domingo-Espín, J.; Corchero, J.L.; Vázquez, E.; Villaverde, A. Microbial Factories for Recombinant Pharmaceuticals. *Microb. Cell Fact.* **2009**, *8*, 17. [CrossRef]
21. Mamat, U.; Wilke, K.; Bramhill, D.; Schromm, A.B.; Lindner, B.; Kohl, T.A.; Corchero, J.L.; Villaverde, A.; Schaffer, L.; Head, S.R.; et al. Detoxifying Escherichia Coli for Endotoxin-Free Production of Recombinant Proteins. *Microb. Cell Fact.* **2015**, *14*, 57. [CrossRef]
22. Carrió, M.M.; Villaverde, A. Protein Aggregation as Bacterial Inclusion Bodies Is Reversible. *FEBS Lett.* **2001**, *489*, 29–33. [CrossRef] [PubMed]
23. Carrió, M.M.; Villaverde, A. Construction and Deconstruction of Bacterial Inclusion Bodies. *J. Biotechnol.* **2002**, *96*, 3–12. [CrossRef] [PubMed]
24. Rosano, G.L.; Ceccarelli, E.A. Recombinant Protein Expression in Escherichia Coli: Advances and Challenges. *Front. Microbiol.* **2014**, *5*, 172. [CrossRef] [PubMed]
25. Sezonov, G.; Joseleau-Petit, D.; D'Ari, R. Escherichia Coli Physiology in Luria-Bertani Broth. *J. Bacteriol.* **2007**, *189*, 8746–8749. [CrossRef] [PubMed]
26. Sahdev, S.; Khattar, S.K.; Saini, K.S. Production of Active Eukaryotic Proteins through Bacterial Expression Systems: A Review of the Existing Biotechnology Strategies. *Mol. Cell. Biochem.* **2008**, *307*, 249–264. [CrossRef] [PubMed]
27. de Marco, A. Protocol for Preparing Proteins with Improved Solubility by Co-Expressing with Molecular Chaperones in *Escherichia coli*. *Nat. Protoc.* **2007**, *2*, 2632–2639. [CrossRef] [PubMed]
28. Upadhyay, V.; Singh, A.; Jha, D.; Singh, A.; Panda, A.K. Recovery of Bioactive Protein from Bacterial Inclusion Bodies Using Trifluoroethanol as Solubilization Agent. *Microb. Cell Fact.* **2016**, *15*, 100. [CrossRef] [PubMed]
29. Simpson, R.J. Solubilization of Escherichia Coli Recombinant Proteins from Inclusion Bodies. *Cold Spring Harb. Protoc.* **2010**, *2010*, 54. [CrossRef]
30. Singh, S.M.; Panda, A.K. Solubilization and Refolding of Bacterial Inclusion Body Proteins. *J. Biosci. Bioeng.* **2005**, *99*, 303–310. [CrossRef]
31. Liu, M.; Wang, B.; Wang, F.; Yang, Z.; Gao, D.; Zhang, C.; Ma, L.; Yu, X. Soluble Expression of Single-Chain Variable Fragment (scFv) in Escherichia Coli Using Superfolder Green Fluorescent Protein as Fusion Partner. *Appl. Microbiol. Biotechnol.* **2019**, *103*, 6071–6079. [CrossRef]
32. Paraskevopoulou, V.; Falcone, F.H. Polyionic Tags as Enhancers of Protein Solubility in Recombinant Protein Expression. *Microorganisms* **2018**, *6*, 47. [CrossRef] [PubMed]
33. Burgess, R.R.; Murray, P. *Deutscher Guide to Protein Purification*; Academic Press: Cambridge, MA, USA, 2009; ISBN 9780080923178.
34. Butt, T.R.; Edavettal, S.C.; Hall, J.P.; Mattern, M.R. SUMO Fusion Technology for Difficult-to-Express Proteins. *Protein Expr. Purif.* **2005**, *43*, 1–9. [CrossRef] [PubMed]
35. Pryor, K.D.; Leiting, B. High-Level Expression of Soluble Protein in Escherichia Coli Using a His6-Tag and Maltose-Binding-Protein Double-Affinity Fusion System. *Protein Expr. Purif.* **1997**, *10*, 309–319. [CrossRef] [PubMed]
36. Smith, D.B.; Johnson, K.S. Single-Step Purification of Polypeptides Expressed in Escherichia Coli as Fusions with Glutathione S-Transferase. *Gene* **1988**, *67*, 31–40. [CrossRef]
37. Ceccarelli, E.A.; Rosano, G.L. *Recombinant Protein Expression in Microbial Systems*; Frontiers: Lausanne, Switzerland, 2014; ISBN 9782889192946.
38. Miladi, B.; El Marjou, A.; Boeuf, G.; Bouallagui, H.; Dufour, F.; Di Martino, P.; Elm'selmi, A. Oriented Immobilization of the Tobacco Etch Virus Protease for the Cleavage of Fusion Proteins. *J. Biotechnol.* **2012**, *158*, 97–103. [CrossRef] [PubMed]
39. Jenny, R.J.; Mann, K.G.; Lundblad, R.L. A Critical Review of the Methods for Cleavage of Fusion Proteins with Thrombin and Factor Xa. *Protein Expr. Purif.* **2003**, *31*, 1–11. [CrossRef] [PubMed]
40. Kuo, D.; Nie, M.; Courey, A.J. SUMO as a Solubility Tag and in Vivo Cleavage of SUMO Fusion Proteins with Ulp1. *Methods Mol. Biol.* **2014**, *1177*, 71–80. [CrossRef]
41. Mészáros, A.; Muwonge, K.; Janvier, S.; Ahmed, J.; Tompa, P. A Novel Tandem-Tag Purification Strategy for Challenging Disordered Proteins. *Biomolecules* **2022**, *12*, 1566. [CrossRef]
42. Barghorn, S.; Biernat, J.; Mandelkow, E. Purification of Recombinant Tau Protein and Preparation of Alzheimer-Paired Helical Filaments in Vitro. *Methods Mol. Biol.* **2005**, *299*, 35–51. [CrossRef]

43. Kronqvist, N.; Rising, A.; Johansson, J. A Novel Approach for the Production of Aggregation-Prone Proteins Using the Spidroin-Derived NT* Tag. *Methods Mol. Biol.* **2022**, *2406*, 113–130. [CrossRef]
44. Abelein, A.; Chen, G.; Kitoka, K.; Aleksis, R.; Oleskovs, F.; Sarr, M.; Landreh, M.; Pahnke, J.; Nordling, K.; Kronqvist, N.; et al. High-Yield Production of Amyloid-β Peptide Enabled by a Customized Spider Silk Domain. *Sci. Rep.* **2020**, *10*, 235. [CrossRef] [PubMed]
45. Mizoguchi, I.; Ooe, Y.; Hoshino, S.; Shimura, M.; Kasahara, T.; Kano, S.; Ohta, T.; Takaku, F.; Nakayama, Y.; Ishizaka, Y. Improved Gene Expression in Resting Macrophages Using an Oligopeptide Derived from Vpr of Human Immunodeficiency Virus Type-1. *Biochem. Biophys. Res. Commun.* **2005**, *338*, 1499–1506. [CrossRef]
46. Chen, G.; Andrade-Talavera, Y.; Tambaro, S.; Leppert, A.; Nilsson, H.E.; Zhong, X.; Landreh, M.; Nilsson, P.; Hebert, H.; Biverstål, H.; et al. Augmentation of Bri2 Molecular Chaperone Activity against Amyloid-β Reduces Neurotoxicity in Mouse Hippocampus in Vitro. *Commun. Biol.* **2020**, *3*, 32. [CrossRef]
47. Orekhov, V.Y.; Jaravine, V.A. Analysis of Non-Uniformly Sampled Spectra with Multi-Dimensional Decomposition. *Prog. Nucl. Magn. Reson. Spectrosc.* **2011**, *59*, 271–292. [CrossRef] [PubMed]
48. Delaglio, F.; Grzesiek, S.; Vuister, G.W.; Zhu, G.; Pfeifer, J.; Bax, A. NMRPipe: A Multidimensional Spectral Processing System Based on UNIX Pipes. *J. Biomol. NMR* **1995**, *6*, 277–293. [CrossRef] [PubMed]
49. Vranken, W.F.; Boucher, W.; Stevens, T.J.; Fogh, R.H.; Pajon, A.; Llinas, M.; Ulrich, E.L.; Markley, J.L.; Ionides, J.; Laue, E.D. The CCPN Data Model for NMR Spectroscopy: Development of a Software Pipeline. *Proteins* **2005**, *59*, 687–696. [CrossRef]
50. Jo, B.H. An Intrinsically Disordered Peptide Tag That Confers an Unusual Solubility to Aggregation-Prone Proteins. *Appl. Environ. Microbiol.* **2022**, *88*, e0009722. [CrossRef]
51. Leonhardt, F.; Gennari, A.; Paludo, G.B.; Schmitz, C.; da Silveira, F.X.; Moura, D.C.D.A.; Renard, G.; Volpato, G.; Volken de Souza, C.F. A Systematic Review about Affinity Tags for One-Step Purification and Immobilization of Recombinant Proteins: Integrated Bioprocesses Aiming Both Economic and Environmental Sustainability. *3 Biotech* **2023**, *13*, 186. [CrossRef] [PubMed]
52. Avila, J.; Medina, M. *Untangling the Role of Tau in Physiology and Pathology*; Frontiers: Lausanne, Switzerland, 2020; ISBN 9782889638352.
53. Götz, J.; Halliday, G.; Nisbet, R.M. Molecular Pathogenesis of the Tauopathies. *Annu. Rev. Pathol.* **2019**, *14*, 239–261. [CrossRef]
54. Corsi, A.; Bombieri, C.; Valenti, M.T.; Romanelli, M.G. Tau Isoforms: Gaining Insight into Alternative Splicing. *Int. J. Mol. Sci.* **2022**, *23*, 15383. [CrossRef]
55. Bhatwa, A.; Wang, W.; Hassan, Y.I.; Abraham, N.; Li, X.-Z.; Zhou, T. Challenges Associated With the Formation of Recombinant Protein Inclusion Bodies in and Strategies to Address Them for Industrial Applications. *Front. Bioeng. Biotechnol.* **2021**, *9*, 630551. [CrossRef]
56. Li, Z.; Nimtz, M.; Rinas, U. The Metabolic Potential of Escherichia Coli BL21 in Defined and Rich Medium. *Microb. Cell Fact.* **2014**, *13*, 45. [CrossRef]
57. Combs, B.; Tiernan, C.T.; Hamel, C.; Kanaan, N.M. Production of Recombinant Tau Oligomers in Vitro. *Methods Cell Biol.* **2017**, *141*, 45–64. [CrossRef]
58. van Swieten, J.; Spillantini, M.G. Hereditary Frontotemporal Dementia Caused by Tau Gene Mutations. *Brain Pathol.* **2007**, *17*, 63–73. [CrossRef]
59. Wang, K.-W.; Zhang, G.; Kuo, M.-H. Frontotemporal Dementia P301L Mutation Potentiates but Is Not Sufficient to Cause the Formation of Cytotoxic Fibrils of Tau. *Int. J. Mol. Sci.* **2023**, *24*, 14996. [CrossRef]
60. Venkatramani, A.; Panda, D. Regulation of Neuronal Microtubule Dynamics by Tau: Implications for Tauopathies. *Int. J. Biol. Macromol.* **2019**, *133*, 473–483. [CrossRef]
61. Kadavath, H.; Hofele, R.V.; Biernat, J.; Kumar, S.; Tepper, K.; Urlaub, H.; Mandelkow, E.; Zweckstetter, M. Tau Stabilizes Microtubules by Binding at the Interface between Tubulin Heterodimers. *Proc. Natl. Acad. Sci. USA* **2015**, *112*, 7501–7506. [CrossRef]
62. Frappier, T.F.; Georgieff, I.S.; Brown, K.; Shelanski, M.L. Tau Regulation of Microtubule-Microtubule Spacing and Bundling. *J. Neurochem.* **1994**, *63*, 2288–2294. [CrossRef]
63. Weingarten, M.D.; Lockwood, A.H.; Hwo, S.Y.; Kirschner, M.W. A Protein Factor Essential for Microtubule Assembly. *Proc. Natl. Acad. Sci. USA* **1975**, *72*, 1858–1862. [CrossRef] [PubMed]
64. Gulisano, W.; Maugeri, D.; Baltrons, M.A.; Fà, M.; Amato, A.; Palmeri, A.; D'Adamio, L.; Grassi, C.; Devanand, D.P.; Honig, L.S.; et al. Role of Amyloid-β and Tau Proteins in Alzheimer's Disease: Confuting the Amyloid Cascade. *J. Alzheimer Dis.* **2018**, *64*, S611–S631. [CrossRef] [PubMed]
65. von Bergen, M.; Barghorn, S.; Li, L.; Marx, A.; Biernat, J.; Mandelkow, E.M.; Mandelkow, E. Mutations of Tau Protein in Frontotemporal Dementia Promote Aggregation of Paired Helical Filaments by Enhancing Local Beta-Structure. *J. Biol. Chem.* **2001**, *276*, 48165–48174. [CrossRef]
66. Mo, Z.-Y.; Zhu, Y.-Z.; Zhu, H.-L.; Fan, J.-B.; Chen, J.; Liang, Y. Low Micromolar Zinc Accelerates the Fibrillization of Human Tau via Bridging of Cys-291 and Cys-322. *J. Biol. Chem.* **2009**, *284*, 34648–34657. [CrossRef]
67. Parolini, F.; Tira, R.; Barracchia, C.G.; Munari, F.; Capaldi, S.; D'Onofrio, M.; Assfalg, M. Ubiquitination of Alzheimer's-Related Tau Protein Affects Liquid-Liquid Phase Separation in a Site- and Cofactor-Dependent Manner. *Int. J. Biol. Macromol.* **2022**, *201*, 173–181. [CrossRef]

68. Prince, P.R.; Hochmair, J.; Brognaro, H.; Gevorgyan, S.; Franck, M.; Schubert, R.; Lorenzen, K.; Yazici, S.; Mandelkow, E.; Wegmann, S.; et al. Initiation and Modulation of Tau Protein Phase Separation by the Drug Suramin. *Sci. Rep.* **2023**, *13*, 3963. [CrossRef]
69. Barré, P.; Eliezer, D. Structural Transitions in Tau k18 on Micelle Binding Suggest a Hierarchy in the Efficacy of Individual Microtubule-Binding Repeats in Filament Nucleation. *Protein Sci.* **2013**, *22*, 1037–1048. [CrossRef]
70. Ferrari, L.; Rüdiger, S.G.D. Recombinant Production and Purification of the Human Protein Tau. *Protein Eng. Des. Sel.* **2019**, *31*, 447–455. [CrossRef]

Disclaimer/Publisher's Note: The statements, opinions and data contained in all publications are solely those of the individual author(s) and contributor(s) and not of MDPI and/or the editor(s). MDPI and/or the editor(s) disclaim responsibility for any injury to people or property resulting from any ideas, methods, instructions or products referred to in the content.